J. Biomechanics Vol. 22, No. 8/9, pp. 853–861, 1989.
Printed in Great Britain

0021-9290/89 $3.00 + .00
Pergamon Press plc

BIPHASIC INDENTATION OF ARTICULAR CARTILAGE—II. A NUMERICAL ALGORITHM AND AN EXPERIMENTAL STUDY

V. C. MOW,* M. C. GIBBS,† W. M. LAI,* W. B. ZHU* and K. A. ATHANASIOU*

*Departments of Mechanical Engineering and Orthopaedic Surgery, Columbia University, New York, NY 10032, U.S.A., †Albany Medical College, Albany, NY 12208, U.S.A.

Abstract—Part I (Mak *et al.*, 1987, *J. Biomechanics* **20**, 703–714) presented the theoretical solutions for the biphasic indentation of articular cartilage under creep and stress-relaxation conditions. In this study, using the creep solution, we developed an efficient numerical algorithm to compute all three material coefficients of cartilage *in situ* on the joint surface from the indentation creep experiment. With this method we determined the average values of the aggregate modulus, Poisson's ratio and permeability for young bovine femoral condylar cartilage *in situ* to be $H_A = 0.90$ MPa, $\nu_s = 0.39$ and $k = 0.44 \times 10^{-15}$ m^4/Ns respectively, and those for patellar groove cartilage to be $H_A = 0.47$ MPa, $\nu_s = 0.24$, $k = 1.42 \times 10^{-15}$ m^4/Ns. One surprising finding from this study is that the *in situ* Poisson's ratio of cartilage (0.13–0.45) may be much less than those determined from measurements performed on excised osteochondral plugs (0.40–0.49) reported in the literature. We also found the permeability of patellar groove cartilage to be several times higher than femoral condyle cartilage. These findings may have important implications on understanding the functional behavior of cartilage *in situ* and on methods used to determine the elastic moduli of cartilage using the indentation experiments.

INTRODUCTION

Numerous studies on the indentation behavior of articular cartilage have been reported in the literature. In some studies, attempts were made to determine the material coefficients describing the mechanical behavior of this tissue *in situ* on the joint surface. Each of these studies had to make a number of *a priori* assumptions on the mechanical behavior of cartilage in order to calculate its *in situ* material coefficients from the results of indentation tests. The common assumptions used to model the 'instantaneous' and 'equilibrium' indentation behavior of articular cartilage are that cartilage is a single phase, linear, isotropic, homogeneous, elastic solid (Hirsch, 1944; Sokoloff, 1966; Kempson *et al.*, 1971a, b; Parsons and Black, 1977; Hoch *et al.*, 1983). From this, in effect, these investigators assumed that two material moduli are adequate to completely describe the instantaneous and equilibrium behavior of cartilage—Young's modulus (E_s) and Poisson's ratio (ν_s) or any two other equivalent coefficients such as aggregate modulus (H_A) and shear modulus (μ_s).‡ In addition, the mathematical solutions for the indentation problem used by most of these investigators were those derived by Hertz (1882) and Hayes *et al.* (1972), which further assumed the conditions of infinitesimal strain and frictionless indenter tip. In light of our present understanding of cartilage biphasic behavior (e.g. Mow *et al.*, 1980, 1982, 1984; Lee *et al.*, 1981; Hoch *et al.*, 1983), we wish to extend the analysis of the indentation experiment to include the effects of interstitial fluid flow by using the linear KLM biphasic model for articular cartilage. In this model, we assume that three material properties—E_s, ν_s and k (permeability)—are adequate to describe the instantaneous, equilibrium and time dependent indentation behavior of cartilage (Mow *et al.*, 1982; Mak *et al.*, 1987). We emphasize here, as with all previous investigations, that we will also assume the conditions of isotropy, homogeneity, infinitesimal strain and frictionless indenter tip. Applications of the present indentation solution—based upon these assumptions—are necessary first steps toward developing even more refined theories which take into account tissue anisotropy, inhomogeneity and material nonlinearities if required by the experimental data.

Using the mathematical solution for the biphasic indentation problem, Mow *et al.* (1982) showed that the elasticity solution derived by Hayes *et al.* (1972) can be used to represent the response of a layer of cartilage in the asymptotic time limits of $t = 0^+$ and $t \to \infty$. In the $t = 0^+$ limit, the instantaneous response of the biphasic medium is identical to that of an incompressible elastic solid ($\nu = 0.5$)§ and in the $t \to \infty$ limit, the equilibrium elastic coefficients E_s and ν_s are those of the porous-permeable solid matrix. However, the problem associated with using only the instantaneous data ($t = 0^+$) and equilibrium data ($t \to \infty$) is that this approach does not describe the observed time-dependent creep or stress-relaxation indentation behaviors of the tissue (Sokoloff, 1966; Kempson *et al.*, 1971a, b; Parsons and Black, 1977; Hoch *et al.*, 1983).

Received in final form 26 *September* 1988.

‡We use the same notation as that adopted by Mak *et al.* (1987), where the subscript s denotes the properties associated with the solid matrix and $H_A = \lambda_s + 2\mu_s$.

§The symbol ν without the subscript s denotes the Poisson's ratio for the single phase linear elasticity model for cartilage.

In an attempt to address this problem, Parsons and Black (1977), following a procedure employed earlier by Hayes and Mockros (1971) and Colleti *et al.* (1972), used a generalized spring–dashpot rheological model to describe the viscoelastic creep behavior of the tissues under indentation conditions. In the present investigation, we propose to use the biphasic indentation analysis of Mak *et al.* (1987) to describe the time-dependent indentation creep behavior of cartilage *in situ*.

An additional difficulty exists in using the indentation data to determine E_s or ν_s of articular cartilage *in situ* from the single phase linear elastic model. This difficulty derives from the fact that an accurate value of ν_s must be known *a priori* when using the Hertz or Hayes *et al.* elasticity solutions. In some earlier studies, the Poisson's ratio ν was simply assumed to be 0.5 (Hirsch, 1944; Sokoloff, 1966; Kempson *et al.*, 1971a, b). In the Parsons and Black studies (1977) the authors showed the 'internal consistency' of the Hayes *et al.* (1972) elasticity theory with the experimental data by plotting the calculated values of the 'geometric scaling function $\kappa(a/h, \nu)$' against the area–aspect ratio a/h for $\nu=0.4$. This value was also assumed by Hoch *et al.* (1983) in their study of biomechanical and biochemical changes in rabbit tibial plateau cartilage even though values as high as 0.44 were determined on excised osteochondral plugs. Finally, Jurvelin *et al.* (1987) showed, by using different diameter solid indenter tips, that the most consistent results for the calculated instantaneous and equilibrium shear moduli were obtained by assuming $\nu=0.4$.

In this study, we show how the biphasic creep indentation solution may be described by a similarity principle and how this principle can be used to determine ν_s and k of articular cartilage from a time-dependent biphasic creep indentation experiment. Using this, we developed a method to calculate all three coefficients (H_A, ν_s, k) associated with the linear KLM biphasic theory for articular cartilage without any *a priori* assumptions as to the values of these coefficients. The reader is referred to Mak *et al.* (1987) for the complete derivation of the mathematical solution used in this study. Below we list only those equations required by us to develop the numerical algorithm.

METHOD OF SOLUTION

The creep displacement of cartilage, $u(t)$, resulting from a Heaviside step loading function, $P_0H(t)$, applied onto the surface of cartilage via an indenter was solved by Mak *et al.* (1987). For an idealized free-draining, porous–permeable, frictionless indenter of radius a, this loading is related to the surface traction by the relationship:

$$P(t) = -\iint_A \sigma^s_{zz}\,dA, \quad z=0, \quad 0\le r\le a, \quad 0\le t<\infty \tag{1}$$

where $z=0$ defines the articular surface. In terms of the Laplace transform solution $g(\gamma, s)$ of the biphasic indentation problem, the loading function $P(t) = P_0H(t)$ is given by:

$$P_0 = -4\pi\mu_s a^2 s\int_0^1 g(\gamma, s)\,d\gamma \tag{2}$$

where the integrand is defined by the solution of the following Fredholm integral equation for the Laplace transform solution creep $\bar{u}(s)$:

$$g(r', s) - \frac{1}{\pi}\int_0^1 [m(\gamma - r', s) + m(\gamma + r', s)]\, g(\gamma, s)\,d\gamma = -\frac{2}{\pi}\bar{u}(s)\left(1 - \frac{1}{2\eta_s}\right). \tag{3}$$

The kernel $m(x, s)$ of this integral equation is given by

$$m(x, s) \equiv \int_0^\infty \left[1 - \xi\left(1 - \frac{1}{2\eta_s}\right) L(\xi, s)\right]\cos(\xi x)\,d\xi \tag{4}$$

where L is a known function, the coefficient $\eta_s = (\lambda_s + 2\mu_s)/2\mu_s$, and λ_s and μ_s are the Lame's coefficients of the solid matrix. It is important to note that η_s may be expressed entirely in terms of the Poisson's ratio ν_s given by $\eta_s = (1-\nu_s)/(1-2\nu_s)$.

Using Simpson's rule of discretization, the solution of the set of Fredholm integral equation, equations (3) and (4), may be reduced to solutions of a set of linear algebraic equations given by:

$$[M][g] = -\frac{2}{\pi}\left[1 - \frac{1}{2\eta_s}\right]\bar{u}(s)[\mathbf{1}]. \tag{5a}$$

Here $g_j = g(r'_j, s)$, and $[\mathbf{1}]$ is the column vector defined by $[1, 1, \ldots, 1]^T$. The matrix $[M]$ is defined by the left side of equation (3) and is given by

$$M_{ij} = \delta_{ij} - \frac{1}{\pi} w_j [m(\gamma_j - r'_i, s) + m(\gamma_j + r'_i, s)] \tag{6}$$

where w_j are the Simpson's weights and δ_{ij} is the Kronecker delta. The corresponding discretization of equation (2) yields:

$$P_0 = -4\pi\mu_s a^2 s[w]^T[g], \tag{7}$$

where $[w]^T$ is the vector of w_j. The Laplace transform solution of the creep solution $\bar{u}(s)$ is determined by the following scheme.

(1) Let $[g*]$ denote the solution of equation (5a) with the right-hand side of the equation replaced by column vector $[\mathbf{1}]$, i.e.

$$[M][g*] = [\mathbf{1}]. \tag{5b}$$

Solve for $[g*]$ using a numerical matrix inversion procedure.

(2) Compute $[g]$ from the expression

$$[g]=-\frac{2}{\pi}\left[1-\frac{1}{2\eta_s}\right]\bar{u}(s)[g*]. \tag{8}$$

(3) Substitution of $[g]$ into equation (7) yields $\bar{u}(s)$ given by the following expression:

$$\bar{u}(s)=\frac{P_0\eta_s}{4s\mu_s a^2(2\eta_s-1)[\mathbf{w}]^T[g*]}. \tag{9}$$

Equation (9) defines the Laplace transform solution of the biphasic creep problem; its inverse provides the creep response for the indenter under the action of the compressive load $P(t)=P_0H(t)$.

NUMERICAL ALGORITHM

Extensive computations are required to obtain a numerical inversion of the matrix equations, equations (5)–(8), and the numerical inversion of the Laplace transform solution for the creep displacement, equation (9). We found that standard IMSL routines cannot be used effectively in an iterative curve-fitting scheme. However, an efficient and fast numerical algorithm can be developed by using the fact that the theoretical indentation creep solution depends on the similarity variable $t'=t/(a^2/kH_A)$ and three dimensionless parameters:

(1) $P_0/(2\mu_s a^2)$—the indenting load;

(2) a/h—the aspect ratio;

(3) ν_s—the Poisson's ratio of the solid matrix.

The ratio a^2/kH_A defines the characteristic time of the biphasic material (Holmes *et al.*, 1985). Figure 1 shows the creep solution for two different values of a^2/kH_A. The dependence of the creep solution on this particular dimensionless time t' means that for a given set of values of $(P_0/2\mu_s a^2, a/h, \nu_s)$, the creep solution $u(t')$ gives the solution $u(t)$ where t is the dimensional time at $a^2/kH_A=1$. Thus, $u(t')$ provides the 'master solutions' for the given set of $(P_0/2\mu_s a^2, a/h, \nu_s)$ from which similar solutions $u(t)$, for other values of a^2/kH_A, can be obtained by shifting the master solution along the logarithmic time axis (Fig. 1).* The amount of shift is given by:

$$\log_{10}(t)-\log_{10}(t')=S \tag{10a}$$

(see Fig. 2). From the definition of t', this shift-factor (S) is given by

$$S=\log_{10}(a^2/kH_A). \tag{10b}$$

The solution of the indentation creep $u(t')$ may be expressed as a function $f[\ ]$ of the four dimensionless variables defined above:

$$u(t')/h=f[t'; P_0/(2\mu_s a^2), a/h, \nu_s]. \tag{11a}$$

The function $f[\ ]$, depending on the dimensionless time t', may be rewritten as a function $G[\ ]$ depending on $\log_{10}(t)$ and S by using equations (10a) and (10b). In so doing, we obtain:

$$u[\log_{10}(t), S]/h=G[\log_{10}(t); S, P_0/(2\mu_s a^2), a/h, \nu_s]. \tag{11b}$$

For any specified values of the load, $P_0/(2\mu_s a^2)$, aspect ratio, a/h, and Poisson's ratio, ν_s, the function G is thus a known function of $\log_{10}(t)$ and S. Finally, the expression for the equilibrium ($t'\to\infty$) creep result is required. This is given by the expression:

$$\frac{u(\infty)}{h}=\frac{a}{h}\left[\frac{P_0}{2a^2\mu_s}\right]\left[\frac{(1-\nu_s)}{2\kappa(a/h,\nu_s)}\right]. \tag{12}$$

Values of κ were numerically tabulated by Hayes *et al.* (1972) for six values of Poisson's ratio from 0.3 to 0.5 and 15 values of a/h from 0.2 to 8. For our purposes, we need the values of κ for all values of ν_s including those between 0 and 0.3. These are obtained from our numerical inverse Laplace transform solution of equation (9).

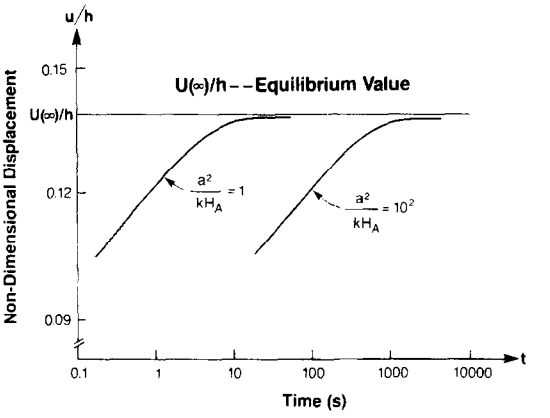

Fig. 1. Representation of theoretical displacement curves for two values of characteristic time $a^2/kH_A=1.0$ and 10^2.

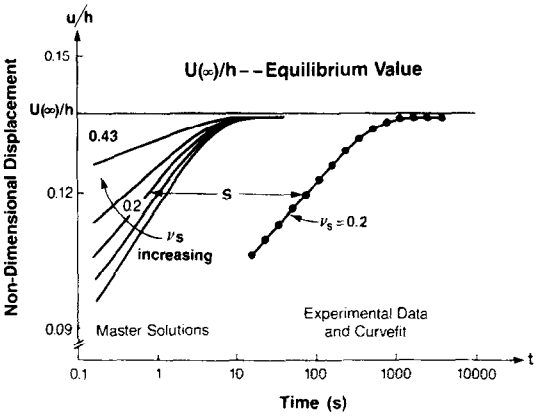

Fig. 2. Schematic depiction of the time-shift method where a master solution is shifted by an amount S along the $\log_{10}(t')$ axis. Diagram illustrates how the 'shape' of the displacement curve is controlled by the parameter ν_s for a given set of P_0, $u(\infty)$, a/h.

*Since $u(t')$ depends linearly on $P_0/2\mu_s a^2$, only master solutions for $P_0/2\mu_s a^2=1$ need to be obtained.

BICUBIC SPLINE FUNCTION REPRESENTATION OF THE MASTER SOLUTION

First, note that the equilibrium data (for any load P_0 and aspect ratio a/h) and equation (12) define a transcendental equation relating μ_s and ν_s. This constraint equation reduces the theoretical time dependent creep response, equation (11b), to depend only on two parameters ν_s and S. Thus, the master solution of the indentation creep problem, defined by setting $S=0$ in equation (11b), depends only on one parameter, ν_s, and the independent variable time. Mak *et al.* (1987) have shown that the inverse Laplace transform procedure used to determine the creep solution requires extensive computations. For experimental purposes, a numerically efficient alternative representation of the master solution for creep indentation is needed. To do this, we used bicubic spline functions (Mortenson, 1985; Coons, 1967) to provide a simple representation of the master solution—denoted by G_b—in the (ν_s,t) plane.

The numerical algorithm we have developed is based upon the construction of a continuous representation of the master solution, $u[\log_{10}(t), 0; \nu_s]$, in the (ν_s, t) plane. We first determined the master solution for a discrete set of (ν_s, t) by calculating the value of μ_s using equation (12) at specified values of $(P_0, u(\infty), a/h)$ at ten values of $\nu_s=(0, 0.05, 0.1, 0.15, \ldots, 0.499)$. Corresponding to each set of values of $(P_0/2\mu_s a^2, a/h, \nu_s)$, master solutions were then determined at 15 discrete values of $\log_{10}(t)$ using equation (11b). This procedure provides a discretized representation of the master solution in the (ν_s, t) plane for a given a/h, with $(P_0/2\mu_s a^2)$ as the parameter.* Because of the simplicity of the bicubic functions, it may be used in curve-fitting procedures where repetitive calculations are required.

CURVE-FITTING PROCEDURE

To curve-fit the experimental data, the least squares sum of the differences, with respect to ν_s and S, between the bicubic spline function representation of the indentation creep solution, G_b, and the experimental data, u_{exp}, is minimized. This means that the sum Q defined by

$$Q=\sum_{t_j}\left\{\frac{G_b[\log_{10}(t_j);S,\nu_s;P_0/2\mu_s a^2,a/h]-[u(\log_{10}(t_j))/h]_{exp}}{u[(\log_{10}(t_j))/h]_{exp}}\right\}^2 \qquad (13)$$

must be minimized with respect to ν_s and S.

Figure 2 illustrates how this minimization procedure works. First, we observe that for given values of P_0, $u(\infty)$ and a/h, the 'shape' of the indentation creep curve, i.e. u vs $\log_{10}(t)$, depends only on ν_s. Second, we note that the 'position' in the u vs $\log_{10}(t)$ graph of a real experimental creep curve is shifted along the $\log_{10}(t)$ axis from the master solution by the shift-factor S; equations (10a) and (10b). The shape and position of the master solution are determined by curve-fitting the experimental creep data using equation (13). From these values of ν_s, S, and μ_s from equation (12), the *in situ* aggregate modulus H_A and the permeability k of the tested cartilage may be calculated from:

$$H_A=2\mu_s(1-\nu_s)/(1-2\nu_s) \quad \text{and} \quad k=(a^2/H_A)10^{-S}. \qquad (14a, b)$$

The Young's modulus E_s of cartilage may also be determined from ν_s and μ_s.

BIPHASIC CREEP INDENTATION APPARATUS

Our new biphasic creep indentation apparatus, Fig. 3, has a variety of features which were specifically designed to facilitate accurate and repeatable testing of cartilage on the joint surface. In this apparatus, the load frame D and loading shaft J are counter-balanced by an adjustable weight C attached to the apex of the loading frame via a steel string hung over a pulley system B supported by two air bearings A. This counter-balance system provides an accurate method of adjusting the tare load (w_t). To adjust the vertical position of the loading frame, a micrometer F is used. The contact between the loading frame D and micrometer tip F forms an electrical contact and is used to monitor the location of the cartilage surface. Contact between the porous–permeable loading tip L (with the tare load w_t) and the cartilage surface M may be obtained by lowering the loading frame D using the micrometer. At the instant contact is made with the articular surface, the electrical circuit between the micrometer tip F and the loading frame D is opened. This position is recorded on an IBM XT which was used both to control the experiment and for data acquisition. The porous indenter tips are made of sintered steel with an average pore size of 44–53 μm and average porosity of 46–51%. The permeability of the porous tip was determined to be at least two to three orders of magnitude higher than that of normal cartilage. For comparison purposes, both porous and solid tipped indenters were used in our creep indentation experiment.

Rapid loading is achieved by lowering the piston attached to a mini-pancake air cylinder fixed inside the housing E. Air pressure provides the motion for the piston and is regulated by an air value. The loading frame D is carefully adjusted to be just below the weight. With careful positioning, a 20–40 ms loading time may be achieved, with little or no inertial overshoot. Unloading is achieved by switching the air

*A table of the bicubic spline function representation of the master solution is available upon request from the first author.

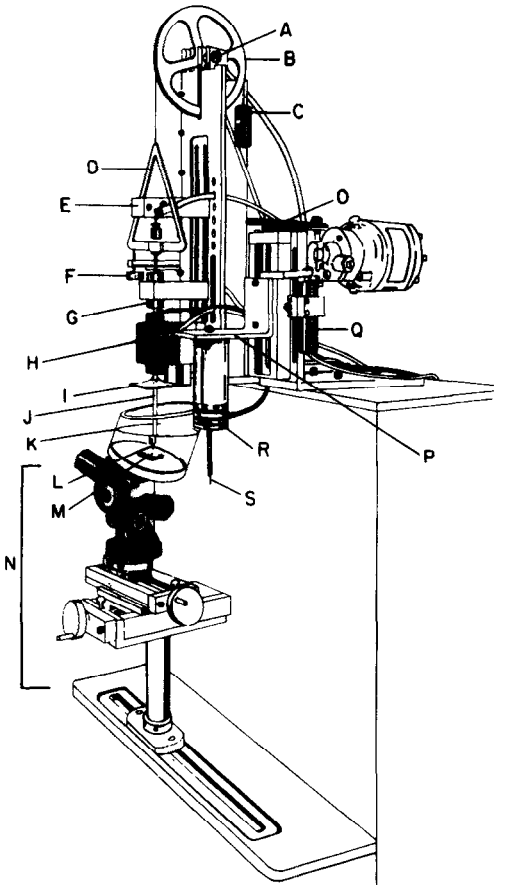

Fig. 3. The biphasic indentation apparatus featuring a porous–permeable indenter tip (L), a six degrees of freedom specimen mounting frame (N) and a thickness measurement probe (S). See text for design and operational details.

valve to raise the weight; thus both creep and recovery curves may be obtained. In addition, because of these features, this apparatus may be used to assess swelling of cartilage against a prescribed tare load in any aqueous solution.

Vertical alignment of the loading shaft may be achieved by adjusting the loading frame D and rectangular linear air bearing H. The rectangular linear air bearing also functions to prevent unwanted rotation of the loading shaft. The test site on the articular surface must be aligned precisely perpendicular to the indenter tip using three unislides for xyz motion and a camera tripod head for θ, ϕ, ψ motion (Fig. 3). Osteochondral specimens are fixed with cyanoacrylate cement to the aluminum base plate of the testing chamber.

The vertical displacement (creep and recovery) of the loading shaft is monitored by a linear variable differential transducer, LVDT, which has a resolution of 12.5 μm and repeatability of 0.5 μm. The LVDT is connected to a signal conditioner whose output is sent to a microcomputer-based data acquisition system. The digitized data are gathered by the IBM XT through appropriate data acquisition programs. Our system is capable of providing variable sampling rates. For the indentation tests, data was sampled at 2 Hz for the first 200 s of both the creep and recovery parts of the experiment, and 0.01 Hz for the remaining time. The digitized signals are transferred to our Micro VAX II for subsequent curve-fitting procedures to determine the material coefficients.

The *in situ* thickness of articular cartilage is determined with a needle probe S similar to those employed by Sokoloff (1966) and Hoch *et al.* (1983) (Fig. 3). With the gimbal design of our apparatus, the thickness of the cartilage may be measured at the exact location and orientation of the test site by the following procedure. Upon completion of an indentation and recovery test, the indentation site of the tissue is marked with India ink. Subsequently, the test chamber K is lowered and the entire gimbal is translated to the right and positioned directly under the needle probe S. This procedure preserves the orientation of the specimen relative to the indentation direction. Measurement of cartilage thickness is achieved by using the load cell R to sense the moment when S penetrates into the cartilage and when S contacts the calcified zone. The displacement of the probe is monitored by the LVDT (Q) which provides the thickness of the tissue at the test site.

TESTING PROCEDURE

Young bovine knee joints were obtained from the abattoir within 24 h of slaughter and kept frozen at −80°C until the day of the indentation test. Each frozen specimen was thawed for 1 h at room temperature in normal saline solution (0.15 M NaCl) containing enzymatic inhibitors (EDTA, 2 mM; benzamidine HCl, 5 mM; N-ethyl malemide, 10 mM and PMSF, 1 mM). Subsequently, the specimen was examined using the India ink staining technique for signs of fibrillation. Only normal joint surfaces were tested. For each indentation test, the specimen was fixed to the base plate of the holder with cyanoacrylate cement. Alignment of the test site was obtained prior to filling the test chamber with solution. Specimens were allowed to equilibrate for 15 min in the solution so that the tissue could regain any fluid loss during the specimen mounting procedure. All porous–permeable indenter tips (1.5 mm in diameter) were ultrasonically cleaned prior to testing to ensure ease of fluid flow into the indenter tip. A tare load w_t of 0.0343 N was applied and the tissue allowed to creep for 14 min prior to the application of the test load w (0.1961 N). These low loads ensured that tissue deformations remained small as required by the infinitesimal strain theory used in the linear biphasic model. Typically, maximum strain values did not exceed 15%. After the test load was applied, specimens were allowed to creep to equilibrium. The time required for the cartilage to reach creep equilibrium may be as long as 10,000 s. With some specimens, solid tip indenters were also used. For this

study, a site along the flat anterior region of the patellar groove, and a site each on the distal posterior medial and anterior lateral condylar surfaces were tested. Three sites on ten bovine knees were studied for 30 indentation tests.

RESULTS

Typical biphasic creep and recovery curves are shown in Fig. 4. Complete recovery is generally observed. This figure illustrates that indentation creep and recovery rates are not identical. This difference in biphasic creep and recovery is consistent and repeatable. Everything else being equal, the difference in the rate of recovery reflects differences in tissue permeability due to compression (Mow *et al.*, 1984; Holmes *et al.*, 1985). In order to explain this, it is necessary to incorporate the nonlinear strain-dependent permeability function into the linear biphasic indentation analysis of Mak *et al.* (1987). Solution to this theoretical problem is not currently available. Using the numerical algorithm described above, the experimental creep curves are curve-fitted to determine the shift-factor S and the Poisson's ratio v_s. The accuracy of a typical curve-fitting result in the logarithmic time is shown in Fig. 5. From this curve-fitting procedure, we determine S and v_s. Once S and v_s are known, the quantities μ_s, H_A, k may be calculated from equations (12), (14a) and (14b). The means and standard deviations of v_s, H_A, k and thickness at the test sites are shown in Table 1.

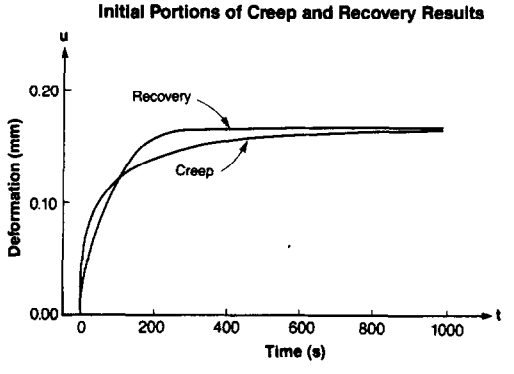

Fig. 4. Comparison of the rate of creep and the rate of recovery in a typical biphasic indentation experiment.

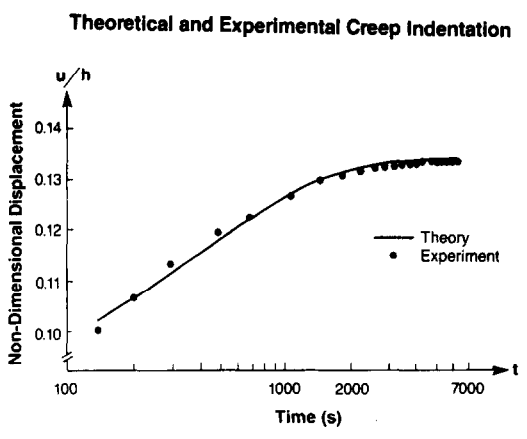

Fig. 5. Typical curve-fits using the master solution G_b for the biphasic creep indentation solution on logarithmic time scale.

The test sites on lateral and medial condyles are probably high weight-bearing areas in bovine knee joints. The test sites on the patellar groove are at the flat central anterior portion of the joint surface and are probably in regions of intermittent loading or low weight-bearing areas. To determine whether any differences exist between the material properties from these three anatomical sites, a one-way analysis of variance (ANOVA) was performed. The ANOVA indicates that there are statistically significant differences in the material properties of cartilage over the bovine joint surface. A Newman–Keuls multiple comparison on means test shows that H_A, v_s, and k of cartilage from the patellar groove differed significantly from those of both condyles, $p<0.05$, while no statistical differences were observed between any of the material properties of medial and lateral condylar cartilages. However, cartilage thickness from the three sites is statistically different, $p<0.05$.

In a previous preliminary investigation, we determined the intrinsic material properties of articular cartilage at 14 sites on six porcine lateral femoral condyles (Whipple *et al.*, 1985). In that study, we found the mean values of H_A, v_s and k to be 0.55 MPa, 0.14 and $2.4\times10^{-15}\,m^4/Ns$, respectively. Thus, the value of H_A, v_s and k for porcine femoral condyle cartilage are different from those of bovine femoral condyle cartilage, suggesting that cartilage properties depend on species.

DISCUSSION AND CONCLUSIONS

The experimental procedure/numerical algorithm presented here describe, for the first time, a method to simultaneously determine all three *in situ* intrinsic material properties (H_A, v_s, k) of articular cartilage as modeled by the linear KLM biphasic theory for isotropic and homogeneous materials. The range of values of the *in situ* aggregate modulus H_A and permeability k are very similar to those determined from the confined compression test of excised human and bovine osteochondral plugs (Mow *et al.*, 1980; Armstrong and Mow, 1982; Mow *et al.*, 1984). Hayes and Mockros (1971) and Hoch *et al.* (1983) reported values of Poisson's ratio of approximately 0.42 which were obtained from excised human and rabbit osteochondral plugs, and values of Poisson's ratio ranging from 0.4 to 0.5 were determined and used by previous investigators to calculate the elastic moduli of articular cartilage using the indentation experiment (Kempson *et al.*, 1971a, b; Hori and Mockros, 1976). However, the present study shows that the Poisson's ratio of young bovine knee joint cartilage varied from 0.13 to 0.45 and this value may depend on the species and

Table 1. Intrinsic properties of bovine knee joint cartilage

Site	ν_s	H_A (MPa)	$k(m^4/Ns)\times 10^{15}$	h (mm)
LC $n=10$	0.40 ± 0.02	0.89 ± 0.29	0.43 ± 0.20	0.94 ± 0.17
MC $n=10$	0.38 ± 0.05	0.90 ± 0.43	0.46 ± 0.33	1.19 ± 0.24
PG $n=10$	0.25 ± 0.07	0.47 ± 0.15	1.42 ± 0.58	1.38 ± 0.19

ν_s, Poisson's ratio; H_A, aggregate modulus; k, permeability; h, tissue thickness at the test site; LC, lateral condyle, MC, medial condyle, PG, patellar groove.

the site tested. Indeed, it may be possible that for some specimens Poisson's ratio approaches zero, as was the case for porcine cartilage (Whipple *et al.*, 1985) and chondroepiphyseal tissue from the femoral heads of human stillborns (Brown and Singerman, 1986). Thus, it is not clear that one can assume *a priori* a specified value for the Poisson's ratio and safely rely on the validity of the calculation for the other elastic moduli.

To illustrate this point, consider the equation relating H_A, μ_s and ν_s given by the identity

$$H_A=\frac{2\mu_s(1-\nu_s)}{(1-2\nu_s)} \tag{15a}$$

and the equilibrium indentation solution

$$H_A=\frac{P_0}{2au(\infty)}\frac{1}{\kappa(a/h,\nu_s)}\frac{(1-\nu_s)^2}{(1-2\nu_s)}. \tag{15b}$$

The dependence of H_A on ν_s from equation (15a) is shown in Fig. 6 for a normalized value of μ_s ($=1$ MPa). Clearly, *a priori* estimates of $\nu_s\to0.5$ will yield considerable errors in calculations for H_A if the actual *in situ* ν_s of cartilage is far from 0.5. It can be easily shown that the calculated aggregate modulus for an assumed Poisson's ratio of 0.42 is about twice that for an assumed value of 0.25.

In addition, from the actual solution of the indentation problem, equation (15b), we may assess the

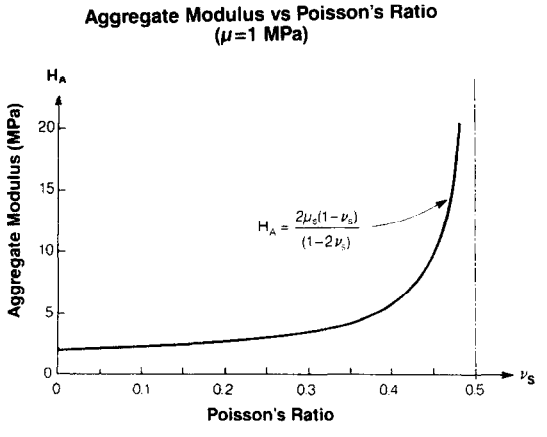

Fig. 6. Theoretical relationship between the aggregate modulus (H_A) and Poisson's ratio (ν_s) of the solid matrix for $\mu_s=1$ MPa.

sensitivity of our calculations for H_A with varying ν_s. For values of κ determined in this study, and for $\Delta\nu_s=0.05$ from $0.30<\nu_s<0.35$, and $0.40<\nu_s<0.45$, we calculate $\Delta H_A=0.08$ and 0.56 MPa, respectively. This sensitivity of H_A with small increments of $\nu_s>0.4$ may be a source of the variation observed in our calculated results (Table 1). Finally, from these estimates of ΔH_A, we can also estimate the sensitivity of k to variations of ν_s for constant S. To do this, we take the differential of k with respect to H_A in equation (10b). This yields the expression

$$\Delta k=-\frac{a^2(\Delta H_A)10^{-S}}{H_A^2}\,. \tag{15c}$$

Inserting typical values of S, H_A and k (Table 1) into this expression yields $10^{-16}<\Delta k<10^{-15}(m^4/Ns)$. Thus, the variations in k found by our method may be due to variations of ν_s. In general, however, the fit between our experimental data and theoretical solution is very good. We believe that a large part of the observed variations in H_A, k, ν_s is due to biological variability of tissue parameters.

Other factors may also play roles in the observed pattern of differences between our theoretical solution and experimental data. We note that the early time response of creep usually differs from the best curve-fit solution (Fig. 5). Also, the linear KLM biphasic theory is not able to account for the observed different rates for creep and recovery. A number of reasons are responsible for these differences. They are undoubtedly based upon the assumptions we made to derive the biphasic indentation creep solution. These assumptions include: (1) inertial effects are negligible; (2) intrinsic viscoelasticity of the solid matrix has negligible effects in compression; (3) the porous–permeable indenter tip is frictionless; (4) cartilage permeability is constant; and (5) the tissue is isotropic and homogeneous. Obviously, these assumptions are not met in any real experiment or for any cartilage.

As specific examples, by neglecting inertial and viscoelastic effects, the creep solution predicts a jump discontinuity of indenter displacement at $t=0^+$ after the load is applied (Mak *et al.*, 1987) while no experimental creep result exhibits such an instantaneous jump. At best, for dead-weight creep devices, the acceleration is limited to that provided by gravity. In

addition, the very nature of a porous–permeable indenter tip will cause interdigitation of the cartilage surface with the rough indenter surface. This interface condition will offer considerable frictional resistance against lateral expansion of the tissue under the indenter tip contrary to our frictionless assumption. Recently, a finite element study has been developed for the linear biphasic theory to address the frictional indenter tip problem (Spilker *et al.*, 1988). This finite element study showed, however, friction at the indenter tip to have small effect on the initial or overall response of the biphasic medium. Also, the assumption of constant permeability (linear biphasic theory) precludes the ability of the theory to predict different creep and recovery rates (Holmes *et al.*, 1985). Finally, the solid tip indenters consistently yield different creep results from those obtained from porous tip indenters. This may be due to squeeze film action developed under the solid indenter tip during the creep process; with a porous tip indenter, fluid exudation from the tissue occurs unimpeded.

In more general terms, other possible causes for differences between our linear KLM biphasic theory for cartilage and indentation analysis and the experimental creep data might be the true anisotropic and inhomogeneous nature of the tissue, strain-dependent permeability and possibility of finite deformation. Indeed, none of these effects were included in the present simplified linear analysis. The general formulation for an anisotropic, inhomogeneous, strain-dependent permeability and finite deformation biphasic theory was, however, derived by Mow *et al.* (1980, 1986). The use of such a general theory in fact could improve upon the predictions of the present linear biphasic model. However, little quantitative information exists as to cartilage anisotropy, inhomogeneity and nonlinearities over the joint surface to render this approach practical. More research needs to be pursued to better define these anisotropies, inhomogeneities and nonlinearities before full advantage of our general biphasic theory can be realized. As a practical matter, nonlinear, anisotropic and inhomogeneous theories should be employed if the experimental data warrants their use (Holmes *et al.*, 1985). In closing, it must be emphasized that the advantage of the present experimental/numerical method is that it obviates the requirement of an *a priori* assumption of Poisson's ratio and provides a method to calculate the *in situ* permeability of cartilage. The values of H_A and k determined by the present method agree well with those obtained from confined compression studies on excised specimens of osteochondral plugs.

Acknowledgements—This work was sponsored by the National Science Foundation, grant no. ECE 85-18501, and the National Institute of Arthritis, Musculoskeletal and Skin Diseases, grant no. AR 38733. The authors wish to thank Drs Barbara A. Best and Mark I. Froimson for their helpful suggestions and editing of the manuscript. Any opinions, findings and conclusions or recommendations expressed in this publication are those of the authors and do not necessarily reflect the views of the National Science Foundation.

REFERENCES

Armstrong, C. G. and Mow, V. C. (1982) Variations in the intrinsic mechanical properties of human articular cartilage with age, degeneration and water content. *J. Bone Jt Surg.* **64A**, 88–94.

Brown, T. D. and Singerman, R. J. (1986) Experimental determination of the linear biphasic constitutive coefficients of human fetal proximal femoral chondroepiphysis. *J. Biomechanics* **19**, 597–605.

Colleti, J. M., Akeson, W. H. and Woo, S. L.-Y. (1972) A comparison of the physical behavior of normal articular cartilage and the arthroplasty surface. *J. Bone Jt Surg.* **54A**, 147–160.

Coons, S. A. (1967) Surface of computer-aided design of space forms. MIT, project MAC-TR-41.

Hayes, W. C., Keer, L. M., Herrmann, G. and Mockros, L. F. (1972) A mathematical analysis for indentation tests of articular cartilage. *J. Biomechanics* **5**, 541–551.

Hayes, W. C. and Mockros, L. F. (1971) Viscoelastic properties of human articular cartilage. *J. appl. Physiol.* **31**, 562–568.

Hertz, H. (1982) Uber die Beruhrung fester elastischer Korper. *J. reine angew. Math., Crelle* **92**, 156.

Hirsch, C. (1944) The pathogenesis of chondromalacia of the patella. *Acta chir. scand.* Suppl. **83**, 1–106.

Hoch, D. H., Grodzinsky, A. J., Koob, T. J., Albert, M. L. and Eyre, D. R. (1983) Early changes in material properties of rabbit articular cartilage after menisectomy. *J. orthop. Res.* **1**, 4–12.

Holmes, M. H., Lai, W. M. and Mow, V. C. (1985) Singular perturbation analysis of the nonlinear flow-dependent, compressive stress–relaxation behavior of articular cartilage. *J. biomech. Engng* **107**, 206–218.

Hori, R. and Mockros, L. F. (1976) Indentation tests of human articular cartilage. *J. Biomechanics* **9**, 259–268.

Jurvelin, J., Kiviranta, I., Aronkoski, J., Tammi, M. and Helminen, H. J. (1987) Indentation study of the biomechanical properties of articular cartilage in canine knee. *Engng Med.* **16**, 16–22.

Kempson, G. E., Freeman, M. A. R. and Swanson, S. A. V. (1971a) The determination of a creep modulus for articular cartilage from indentation tests on the human femoral head. *J. Biomechanics* **4**, 239–250.

Kempson, G. E., Spivey, C. J., Swanson, S. A. V. and Freeman, M. A. R. (1971b) Patterns of cartilage stiffness on normal and degenerate femoral heads. *J. Biomechanics* **4**, 597–609.

Lee, R. C., Frank, E. H., Grodzinsky, A. J. and Roylance, D. K. (1981) Oscillatory compressional behavior of articular cartilage and its associated electrochemical properties. *J. biomech. Engng* **103**, 280–292.

Mak, A. F., Lai, W. M. and Mow, V. C. (1987) Biphasic indentation of articular cartilage—I. Theoretical solution. *J. Biomechanics* **20**, 703–714.

Mortenson, M. E. (1985) *Geometric Modeling.* John Wiley, New York.

Mow, V. C., Holmes, M. H. and Lai, W. M. (1984) Fluid transport and mechanical properties of articular cartilage: a review. *J. Biomechanics* **17**, 377–394.

Mow, V. C., Kuei, S. C., Lai, W. M. and Armstrong, C. G. (1980) Biphasic creep and stress relaxation of articular cartilage. *J. biomech. Engng* **102**, 73–84.

Mow, V. C., Kwan, M. K., Lai, W. M. and Holmes, M. H. (1986) A finite deformation theory for nonlinearly permeable soft hydrated biological tissues. *Frontiers in Bio-*

mechanics (Edited by Schmid-Schonbein, G., Woo, S. and Zweifach, B.), pp. 153–179. Springer, New York.

Mow, V. C., Lai, W. M. and Holmes, M. H. (1982) Advanced theoretical and experimental techniques in cartilage research. *Biomechanics: Principles and Applications* (Edited by Huiskes, R., Van Campen, D. and Dewijn, J.), pp. 47–74. Martinus Nijhoff, The Hague.

Parsons, J. R. and Black, J. (1977) The viscoelastic shear behavior of normal rabbit articular cartilage. *J. Biomechanics* **10**, 21–29.

Sokoloff, L. (1966) Elasticity of aging cartilage. *Proc. Fedn Am. Socs exp. Biol.* **25**, 1089–1095.

Spilker, R. L., Suh, J. K. and Mow, V. C. (1988) A finite element formulation of the nonlinear biphasic model for articular cartilage and hydrated soft tissues including strain-dependent permeability. *Computational Methods in Bioengineering*, (Edited by Spilker, R. L. and Simon, B. R.) ASME BED-Vol. 9, pp. 81–92. ASME, New York.

Whipple, R. R., Gibbs, M. C., Lai, W. M., Mow, V. C., Mak, A. F. and Wirth, C. R. (1985) Biphasic properties of repair cartilage at the articular surface. *Trans. orthop. Res. Soc.* **10**, 340.